

Structural and Vibrational Properties of the Octanuclear Silasesquioxane $C_6H_{13}(H_7Si_8O_{12})^\dagger$

Gion Calzaferri,^{*a} Roman Imhof^a and Karl W. Törnroos^{*b}

^a Institute of Inorganic and Physical Chemistry, University of Berne, CH-3000 Berne 9, Switzerland

^b Structural Chemistry, Stockholm University, S-106 91 Stockholm, Sweden

The crystal structure of hexylheptahydrooctasilasesquioxane $C_6H_{13}(H_7Si_8O_{12})$ has been determined by single-crystal X-ray diffraction and compared with the structures of $H_8Si_8O_{12}$, $[Co(CO)_4(H_7Si_8O_{12})]$ and $(CH_3)_8Si_8O_{12}$. The monosubstituted silasesquioxane molecules have a crystallographic C_1 symmetry. The local symmetry of their octanuclear Si cage, however, is close to C_{3v} . They are closer to C_{3v} than $H_8Si_8O_{12}$ which has an effective molecular symmetry of T_h in the crystal. The major distortions originate in intermolecular $O \cdots Si$ contacts. The larger the number of such contacts per molecule, the larger is the distortion of the local symmetry of the cage. The structure of $C_6H_{13}(H_7Si_8O_{12})$ compares well with that of $[Co(CO)_4(H_7Si_8O_{12})]$, and it is clearly the least distorted of the two due to a reduced influence of the *n*-hexyl ligand on the cage geometry and due to a smaller number of intermolecular interactions. The IR spectrum of $C_6H_{13}(H_7Si_8O_{12})$ has been interpreted by correlating it with the three molecules $H_8Si_8O_{12}$, $C_6H_{13}[Si(OSiMe_3)_3]$ and $HSi(OSiMe_3)_3$.

The highly symmetrical hydrosilasesquioxanes of the general formula $(HSiO_{1.5})_{2n}$, $n = 2, 3, etc.$, are very appealing molecules for studying structural and vibrational properties of compounds with Si–O bonds. The crystal structures of $H_8Si_8O_{12}$,^{1,2} $H_{10}Si_{10}O_{15}$,³ and $H_{12}Si_{12}O_{18}$,⁴ have been studied in detail and the structures of two isomers of $H_{14}Si_{14}O_{21}$ have been reported by Agaskar *et al.*⁵ Among these molecules $H_8Si_8O_{12}$ is of special interest. Its vibrational properties have been investigated and an accurate force field in terms of internal force constants has been determined based on extensive IR and Fourier-transform (FT) Raman data and on a normal coordinate analysis.⁶ Monosubstituted octanuclear spherosilasesquioxanes of the type $RH_7Si_8O_{12}$ [$R =$ alkyl or aryl,⁷ ferrocenyl⁸ or $Co(CO)_4$ ⁹] have become available recently, opening a route to an interesting spherosiloxane chemistry. Until now only one of them, $[Co(CO)_4(H_7Si_8O_{12})]$, has been characterized by single-crystal X-ray diffraction.⁹ These molecules are potential precursors for a new type of polymeric material with organometallic units.¹⁰ We have now succeeded in crystallizing hexylheptahydrooctasilasesquioxane $C_6H_{13}(H_7Si_8O_{12})$ and have studied its crystal structure in comparison to those of $[Co(CO)_4(H_7Si_8O_{12})]$, $H_8Si_8O_{12}$ and $(CH_3)_8Si_8O_{12}$.¹¹ In addition we have measured its IR spectrum and assigned the bands according to group frequencies,^{12,13} the results of a normal coordinate analysis of $H_8Si_8O_{12}$ ⁶ and a comparison with the spectra of $HSi(OSiMe_3)_3$ and $C_6H_{13}[Si(OSiMe_3)_3]$.

Results and Discussion

Synthesis.—The synthesis of $C_6H_{13}(H_7Si_8O_{12})$ started from octahydrooctasilasesquioxane $H_8Si_8O_{12}$ which was dissolved in cyclohexane and refluxed together with hex-1-ene and a catalytic amount of a H_2PtCl_6 solution in Pr^iOH . After evaporation of the solvent the viscous solution was separated on a size-exclusion liquid chromatography column. The solubility of the white product in aprotic solvents is high. Like all the other hydrosilasesquioxanes it is not stable in protic solvents. It was therefore recrystallized from nonane–dichloromethane to give

colourless aggregated flakes. The model substance hexyltris-(trimethylsiloxy)silane $C_6H_{13}[Si(OSiMe_3)_3]$ was prepared by a similar hydrosilylation procedure starting from tris-(trimethylsiloxy)silane $HSi(OSiMe_3)_3$ and hex-1-ene. The product was a highly viscous, colourless liquid which was characterized by ¹H NMR, MS and IR spectroscopy.

Molecular Structure.—The structure of $C_6H_{13}(H_7Si_8O_{12})$, shown in Fig. 1, represents the third octanuclear silasesquioxane molecule which we have characterized by X-ray diffraction. The first was $H_8Si_8O_{12}$,² the second the monosubstituted $[Co(CO)_4(H_7Si_8O_{12})]$.⁹ The structural results on these two compounds therefore serve as a basis of comparison. The crystallographic symmetry of $H_8Si_8O_{12}$ is C_{3i} , but the molecule has a non-crystallographic symmetry, T_h . Both $C_6H_{13}(H_7Si_8O_{12})$ and $[Co(CO)_4(H_7Si_8O_{12})]$ have a molecular symmetry of C_1 . The highest attainable symmetry of the cage fragment itself is, however, O_h . The crystalline state discloses intermolecular interactions which exercise a decisive role on the molecular geometry of these cage compounds. Attention is therefore focussed on the deformations of the cage structure, their nature, magnitudes and origin.

The atomic coordinates of $C_6H_{13}(H_7Si_8O_{12})$ are given in Table 1 and selected bond lengths and angles in Table 2. The most important geometrical features are summarised by the following mean values: the Si–O distance is 1.606(8) Å, the O–Si–O angle is 109.50(29)° when excluding the angles around Si(1), and 109.37(45)° when averaging all O–Si–O angles, the Si–O–Si angle is 148.52(1.73)°. The non-bonding distance of the Si_8 -cube edge is 3.092(13) Å, the corner angles of the cube being 90.00(39)°. The body diagonal Si \cdots Si distances are 5.356(22) Å on average, including Si(1) \cdots Si(4) and 5.345(3) Å excluding Si(1) \cdots Si(4).

The *n*-hexyl group induces the same deformation features on the Si(1) tetrahedron as does the $Co(CO)_4$ group in $[Co(CO)_4(H_7Si_8O_{12})]$, but to a much lesser extent. Thus Si(1) is moved out of the cage, as may be concluded from the mean angles [O–Si(1)–O, 108.51(16)° and C(1)–Si(1)–O 110.42(18)°] as well as from the Si(1) \cdots Si(4) body diagonal distance of 5.388(2) Å. The latter is elongated in relation to the remaining distances, which are the same to within two e.s.d.s. The Si(1)–C(1) distance of 1.832(4) Å is in accord with the mean value of 1.828(5) Å in

† Supplementary data available: see Instructions for Authors, *J. Chem. Soc., Dalton Trans.*, 1994, Issue 1, pp. xxiii–xxviii.

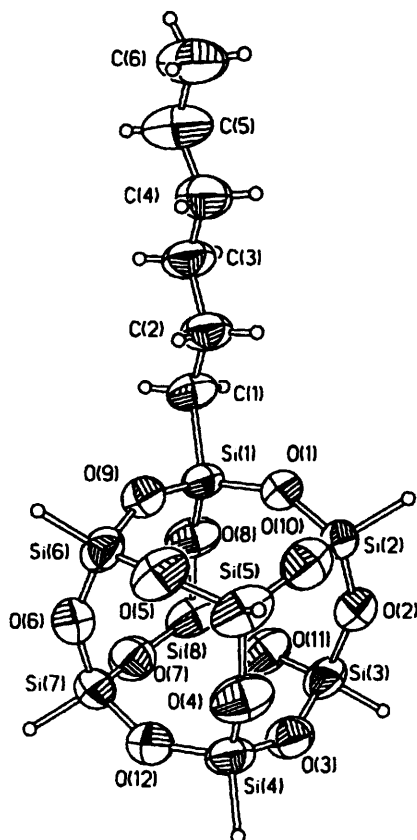


Fig. 1 The crystal structure of $C_6H_{13}(H_7Si_8O_{12})$, displayed with atomic labelling and anisotropic displacement parameters at the 50% probability level

Table 1 Atomic fractional coordinates for $C_6H_{13}(H_7Si_8O_{12})$ with estimated standard deviations (e.s.d.s) in parentheses

Atom	x	y	z
Si(1)	-0.275 85(14)	0.412 27(13)	0.677 56(6)
Si(2)	0.053 30(14)	0.420 32(16)	0.751 30(7)
Si(3)	-0.007 20(16)	0.067 47(14)	0.826 85(7)
Si(4)	-0.233 87(17)	0.232 74(16)	0.966 44(6)
Si(5)	-0.173 11(21)	0.586 54(15)	0.890 77(8)
Si(6)	-0.503 38(16)	0.578 09(15)	0.819 44(7)
Si(7)	-0.564 08(16)	0.225 98(20)	0.893 49(8)
Si(8)	-0.337 42(19)	0.061 70(13)	0.753 45(8)
O(1)	-0.080 2(3)	0.429 4(4)	0.692 6(2)
O(2)	0.079 6(4)	0.230 3(4)	0.784 4(2)
O(3)	-0.096 7(4)	0.111 7(4)	0.911 8(2)
O(4)	-0.189 6(5)	0.425 1(4)	0.948 6(2)
O(5)	-0.359 1(5)	0.635 0(4)	0.864 0(2)
O(6)	-0.592 5(4)	0.419 2(4)	0.863 9(2)
O(7)	-0.486 5(4)	0.109 9(4)	0.823 7(2)
O(8)	-0.319 9(4)	0.218 3(3)	0.693 5(2)
O(9)	-0.411 6(3)	0.527 8(3)	0.736 3(2)
O(10)	-0.023 7(4)	0.541 9(4)	0.819 0(2)
O(11)	-0.154 3(4)	0.014 0(3)	0.782 1(2)
O(12)	-0.429 1(4)	0.213 1(4)	0.952 2(2)
C(1)	-0.294 0(6)	0.482 1(5)	0.580 6(2)
C(2)	-0.239 5(7)	0.660 8(6)	0.559 6(2)
C(3)	-0.275 3(7)	0.729 8(6)	0.483 7(3)
C(4)	-0.219 5(7)	0.907 0(7)	0.463 5(3)
C(5)	-0.276 3(10)	0.985 5(8)	0.394 3(3)
C(6)	-0.220 5(9)	1.159 9(8)	0.374 6(4)

the structure of $(CH_3)_8Si_8O_{12}$.¹¹ Similar to $[Co(CO)_4(H_7Si_8O_{12})]$, the only deformations in the $C_6H_{13}(H_7Si_8O_{12})$ cage which significantly exceed those in $H_8Si_8O_{12}$ concern the $Si(1) \cdots Si(4)$ body diagonal distance, and the tetrahedral

Table 2 Interatomic distances (Å) and angles (°) for $C_6H_{13}(H_7Si_8O_{12})$ excluding the *n*-hexyl group

Si(1)-C(1)	1.832(4)	Si(5)-O(4)	1.612(3)
Si(1)-O(1)	1.614(3)	Si(5)-O(5)	1.612(3)
Si(1)-O(8)	1.617(3)	Si(5)-O(10)	1.603(4)
Si(1)-O(9)	1.609(3)	Si(6)-O(5)	1.607(3)
Si(2)-O(1)	1.607(3)	Si(6)-O(6)	1.609(3)
Si(2)-O(2)	1.606(3)	Si(6)-O(9)	1.592(3)
Si(2)-O(10)	1.591(4)	Si(7)-O(6)	1.612(3)
Si(3)-O(2)	1.614(3)	Si(7)-O(7)	1.594(4)
Si(3)-O(3)	1.604(3)	Si(7)-O(12)	1.614(3)
Si(3)-O(11)	1.616(3)	Si(8)-O(7)	1.588(4)
Si(4)-O(3)	1.599(3)	Si(8)-O(8)	1.606(3)
Si(4)-O(4)	1.608(3)	Si(8)-O(11)	1.607(3)
Si(4)-O(12)	1.610(3)		
O(1)-Si(1)-C(1)	110.4(1)	O(6)-Si(6)-O(9)	109.9(2)
O(1)-Si(1)-O(8)	108.9(2)	O(6)-Si(7)-O(7)	109.6(2)
O(1)-Si(1)-O(9)	108.1(2)	O(6)-Si(7)-O(12)	109.1(2)
O(8)-Si(1)-C(1)	111.0(2)	O(7)-Si(7)-O(12)	109.9(2)
O(8)-Si(1)-O(9)	108.5(2)	O(7)-Si(8)-O(8)	109.7(2)
O(9)-Si(1)-C(1)	109.9(1)	O(7)-Si(8)-O(11)	109.2(2)
O(1)-Si(2)-O(2)	109.5(2)	O(8)-Si(8)-O(11)	110.0(2)
O(1)-Si(2)-O(10)	109.9(2)	Si(1)-O(1)-Si(2)	148.6(2)
O(2)-Si(2)-O(10)	109.2(2)	Si(2)-O(2)-Si(3)	148.6(2)
O(2)-Si(3)-O(3)	109.7(2)	Si(3)-O(3)-Si(4)	147.5(2)
O(2)-Si(3)-O(11)	109.2(2)	Si(4)-O(4)-Si(5)	149.6(2)
O(3)-Si(3)-O(11)	109.6(2)	Si(5)-O(5)-Si(6)	146.7(2)
O(3)-Si(4)-O(4)	109.5(2)	Si(6)-O(6)-Si(7)	146.7(2)
O(3)-Si(4)-O(12)	109.1(2)	Si(7)-O(7)-Si(8)	150.4(2)
O(4)-Si(4)-O(12)	109.4(2)	Si(1)-O(8)-Si(8)	146.6(2)
O(4)-Si(5)-O(5)	109.0(2)	Si(1)-O(9)-Si(6)	152.5(2)
O(4)-Si(5)-O(10)	109.4(2)	Si(2)-O(10)-Si(5)	148.6(2)
O(5)-Si(5)-O(10)	109.8(2)	Si(3)-O(11)-Si(8)	148.5(2)
O(5)-Si(6)-O(6)	109.2(2)	Si(4)-O(12)-Si(7)	148.0(2)
O(5)-Si(6)-O(9)	109.5(2)		

geometry of Si(1). The Si-O-Si angles, α , are inversely proportional to the Si-O distances, d , and the relationship conforms to the equation $d(\text{Si-O}) = 1.59 + [1.6 \times 10^{-8}(180 - \alpha)^4]$, which is slightly modified compared to the equation originally derived from spherosilasesquioxanes.³ The significant deformations occur at the very flexible Si-O-Si angles enabling a co-operative torsional displacement around the R-Si axis of the Si tetrahedra. The non-bonding O(1,5) distances between opposite O atoms associated with the faces of the Si_8 cube, e.g. $O(1) \cdots O(5)$ vs. $O(9) \cdots O(10)$, provide a sensitive measure of the degree of the deformation and its effect on the local cage symmetry. In a cage of O_h symmetry, it is required that the two O atoms in each of the six diagonal mirror planes of the Si_8 cube, lie exactly in their respective planes, i.e. the twelve O(1,5) distances must be equal. The monosubstituted molecules maintain an approximate C_{3v} symmetry, approaching C_{3v} as the deviation of the O atoms from the diagonal mirror planes decreases. The non-bonding O(1,5) distances in $C_6H_{13}(H_7Si_8O_{12})$ show a maximum difference of 0.171(4) Å, to be compared to 0.231(6) Å in $[Co(CO)_4(H_7Si_8O_{12})]$ and 0.307(1) Å in $H_8Si_8O_{12}$. The average absolute departure of the O atoms out of the six diagonal planes of the silicon cube is 0.030(4) Å, while 0.042(3) Å in $[Co(CO)_4(H_7Si_8O_{12})]$ and 0.112(1) Å in $H_8Si_8O_{12}$. The mean departure is -0.003(4) Å, implying that a local C_{3v} symmetry of the cage is present on average. In addition and analogous to this reasoning, the shorter $Si(1) \cdots Si(4)$ body diagonal distance of 5.388(2) Å, compared to 5.411(2) Å in $[Co(CO)_4(H_7Si_8O_{12})]$, indicates an approach of the local symmetry also towards O_h . Clearly, the cage symmetry of $C_6H_{13}(H_7Si_8O_{12})$ lies closer to both C_{3v} and O_h than does $[Co(CO)_4(H_7Si_8O_{12})]$, and on average also closer to C_{3v} symmetry than $H_8Si_8O_{12}$.

A notable difference in $C_6H_{13}(H_7Si_8O_{12})$ compared to the other two molecules concerns the molecular packing where only one short intermolecular contact of the type $O \cdots Si$ less than

3.7 Å is present, 3.677(4) Å, meaning that there are two such contacts per molecule. The corresponding number of contacts for $[\text{Co}(\text{CO})_4(\text{H}_7\text{Si}_8\text{O}_{12})]$ is four, and eight for $\text{H}_8\text{Si}_8\text{O}_{12}$. The number of contacts appears proportional to the magnitude of the out-of-plane deformation of the O atoms and the subsequent distortion of the local symmetry as well as to an increase of the crystal density: 1.55, 1.84 and 1.97 g cm^{-3} for $\text{C}_6\text{H}_{13}(\text{H}_7\text{Si}_8\text{O}_{12})$, $[\text{Co}(\text{CO})_4(\text{H}_7\text{Si}_8\text{O}_{12})]$ and $\text{H}_8\text{Si}_8\text{O}_{12}$ respectively. The pattern of molecular packing is basically the same as for $[\text{Co}(\text{CO})_4(\text{H}_7\text{Si}_8\text{O}_{12})]$, with the *n*-hexyl substituents gathered, forming alternating layers of cages and *n*-hexyl groups throughout the crystal, as illustrated in Fig. 2.

The mean Si...Si body diagonal distance for $(\text{CH}_3)_8\text{Si}_8\text{O}_{12}$ is 5.3917(1) Å, and the Si...Si cube edge 3.1129(4) Å,¹¹ indicating that the cage symmetry of this molecule is T_h to within the experimental error. However, the non-bonding O(1,5) distances show a maximum difference of 0.075(3) Å, revealing a significant deviation from O_h symmetry, although the smallest among the octasilasesquioxane cage structures

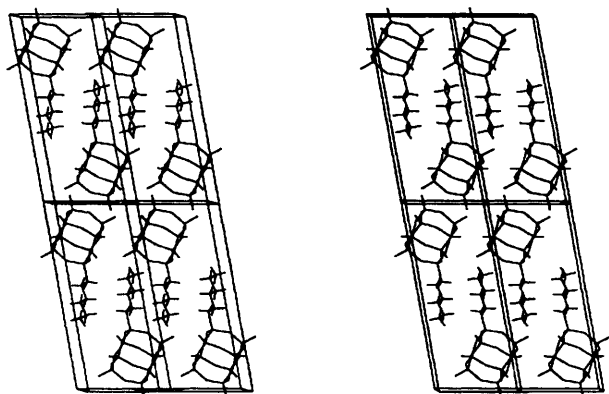


Fig. 2 Stereoscopic illustration of the molecular packing of $\text{C}_6\text{H}_{13}(\text{H}_7\text{Si}_8\text{O}_{12})$, seen normal to the *bc* plane

observed so far. These observations are congruent with the conclusions of the above comparison, in that this molecule lacks short intermolecular $\text{O} \cdots \text{Si}$ contacts below 3.7 Å and also has the lowest crystal density (1.51 g cm^{-3}). Previous studies showed that the intermolecular $\text{O} \cdots \text{Si}$ contacts reflect an incipient nucleophilic attack of oxygen on silicon, resulting in molecular distortions.^{2,3} We find that our analysis clearly establishes the fact that these intermolecular contacts play a crucial role in the distortion of the cage structure and in the subsequent lowering of the molecular symmetry.

Vibrational Structure.—An overview of the IR transmission spectra of $\text{H}_8\text{Si}_8\text{O}_{12}$ and $\text{C}_6\text{H}_{13}(\text{H}_7\text{Si}_8\text{O}_{12})$ is shown in Fig. 3. The spectrum of $\text{H}_8\text{Si}_8\text{O}_{12}$ in solution is fully compatible with the point group O_h and theory predicts six fundamental IR-active vibrations of the symmetry type T_{1u} . The four additional absorptions present in the spectrum are combination bands.⁶ Substitution of one hydrogen by a hexyl group lowers the symmetry to C_1 . This means that no symmetry restrictions should apply and that the spectrum might become complicated. However, the spectrum remains remarkably simple and is dominated by only slightly shifted bands originating from the octanuclear siloxane cage. Therefore it makes sense to discuss the IR spectrum of $\text{C}_6\text{H}_{13}(\text{H}_7\text{Si}_8\text{O}_{12})$ in terms of the well established group frequency approach.

Good group frequencies are based on a large variety of spectra of comparable molecules and on a potential energy distribution (PED) analysis of well chosen model substances. Both conditions are fulfilled here. The vibrational structure of $\text{H}_8\text{Si}_8\text{O}_{12}$ is fully understood and a detailed PED analysis has been carried out for this molecule.⁶ To obtain the missing information concerning the hexyl substituent we have investigated the spectrum of hexyltris(trimethylsiloxy)silane $\text{C}_6\text{H}_{13}[\text{Si}(\text{OSiMe}_3)_3]$ I which represents the substituted edge of the cubic cage of $\text{RH}_7\text{Si}_8\text{O}_{12}$. The superposition of the spectra of these two molecules gives a reasonable basis for the interpretation of the IR spectrum of $\text{C}_6\text{H}_{13}(\text{H}_7\text{Si}_8\text{O}_{12})$.

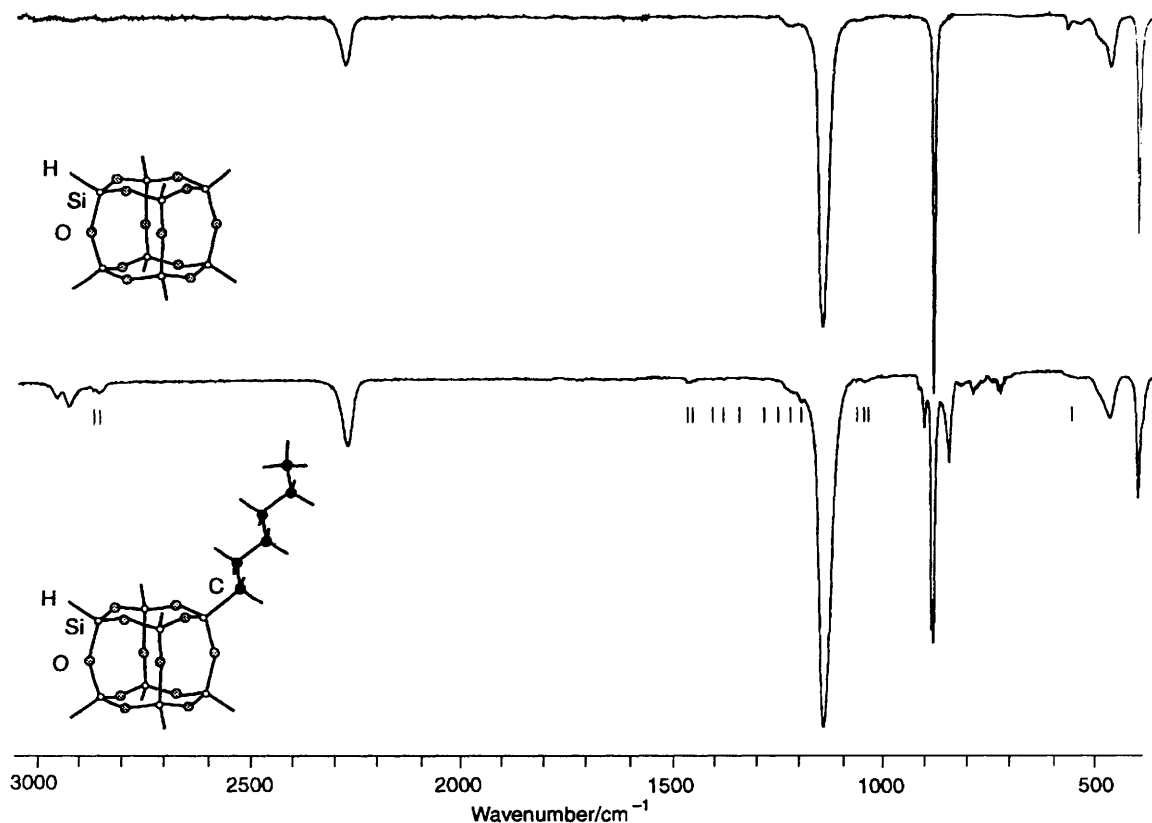


Fig. 3 Overview IR transmission spectra of $\text{H}_8\text{Si}_8\text{O}_{12}$ and $\text{C}_6\text{H}_{13}(\text{H}_7\text{Si}_8\text{O}_{12})$. Bands indicated as very weak in Table 3 are marked by vertical lines

Compound **1** introduces additional trimethylsilyl bands which can be assigned by comparison with the well understood spectrum of $\text{HSi}(\text{OSiMe}_3)_3$ **2**.¹⁴ The results of the band assignment are summarized in Table 3 and discussed below.

3000–2800 cm^{-1} . The silicon atom bound to the C_6H_{13} hexyl group shifts the symmetrical C–H stretching vibrations of the adjacent carbon atom by about 10 cm^{-1} to higher energies with respect to aliphatics.

1500–1370 cm^{-1} . Similar to the stretching vibrations the CH_3 and CH_2 deformation bands are sensitive to the adjacent atoms. Silicon lowers the wavenumber by about 40 cm^{-1} . We therefore assign the weak band at 1467 cm^{-1} to the Si– CH_2 deformation vibration. The bands at 1467 and 1458 cm^{-1} correspond to the remaining CH_3 and the four CH_2 groups.

1350–1150 cm^{-1} . The very weak bands in this region may be

attributed to CH_2 wagging vibrations. The most intense one at 1195 cm^{-1} originates from the CH_2 group bound to the silicon atom in agreement with literature data.¹² The assignment of the very weak band at 1213 cm^{-1} remains uncertain. It could also be attributed to a combination band of the strong antisymmetric Si–O–Si stretch with the low frequency vibration at 84 cm^{-1} in $\text{H}_8\text{Si}_8\text{O}_{12}$.⁶

1065–700 cm^{-1} . The intensities of the skeletal modes in alkanes are weak compared with those of the C–H stretching and deformation vibrations. The only exception is the CH_2 rocking at about 720 cm^{-1} . The intense absorptions between 916 and 882 cm^{-1} are therefore assigned to $\delta(\text{Si-H})$ discussed later. The 790 cm^{-1} absorption can be correlated to Si–C stretching. The nature of the very weak bands at about 1050 cm^{-1} is not clear. Smith¹² reports in this region several bands for

Table 3 Infrared absorptions (cm^{-1}) of $\text{H}_8\text{Si}_8\text{O}_{12}$, $\text{C}_6\text{H}_{13}(\text{H}_7\text{Si}_8\text{O}_{12})$, $\text{C}_6\text{H}_{13}[\text{Si}(\text{OSiMe}_3)_3]$ **1** and $\text{HSi}(\text{OSiMe}_3)_3$ **2** and their assignment (v = very, s = strong, m = medium, w = weak, sh = shoulder, br = broad, sci = scissoring, wag = wagging)

$\text{H}_8\text{Si}_8\text{O}_{12}$	$\text{C}_6\text{H}_{13}(\text{H}_7\text{Si}_8\text{O}_{12})$	1	2	Assignment ^{6,12-14}
	2959w	2959s	2960s	$\nu_{\text{asym}}(\text{CH}_3)$
	2930w	2927s		$\nu_{\text{asym}}(\text{CH}_2)$
		2901m	2898m	$\nu_{\text{sym}}(\text{CH}_3)\text{-Si}$
	2873vw	2873m		$\nu_{\text{sym}}(\text{CH}_2)\text{-Si}$
	2862vw	2859m		$\nu_{\text{sym}}(\text{CH}_2)$
2277m	2274m		2201m	$\nu(\text{Si-H})$
	1467vw	1468w		$\delta_{\text{sci}}(\text{CH}_2)/\delta_{\text{asym}}(\text{CH}_3)$
	1458vw	1457w		
		1453 (sh)	1454w	
		1442vw	1439w	$\delta_{\text{asym}}(\text{CH}_3)\text{-Si}$
		1413w	1414m	
		1404w	1403m	
	1407vw			$\delta_{\text{sci}}(\text{CH}_2)\text{-Si}$
	1379vw	1378vw		$\delta_{\text{sym}}(\text{CH}_3)$
	1349vw	1342vw	1334w	
	1286vw			$\rho_{\text{wag}}(\text{CH}_2)$
		1260vs	1261vs	$\delta_{\text{sym}}(\text{CH}_3)\text{-Si}$
		1251vs	1253vs	
	1250vw	1230 (sh)		$\rho_{\text{wag}}(\text{CH}_2)$
	1213vw			
1215vw		1191w		Combination band
	1195w			$\rho_{\text{wag}}(\text{CH}_2)\text{-Si}$
1141vs	1139vs			
		1100 (sh)	1100 (sh)	$\nu_{\text{asym}}(\text{Si-O-Si})$
		1057vs	1065vs	Combination band
1065vw				
	1064vw			
	1047vw			$\nu(\text{C-C})$
	1040vw			
	916w			
	905m			
881vs	887vs		907s	$\delta(\text{Si-H})$
	882vs			
	847m			Not assigned
		866vs		
		845vs	846vs	$\rho_{\text{rock}}[\text{Si}(\text{CH}_3)_3]$
	817w			Not assigned
	790w	790w	791w	$\nu(\text{Si-C})$
		756s	756s	
	716w	710w	724vw	$\rho_{\text{rock}}(\text{CH}_2)$
		685w	689w	$\nu_{\text{asym}}(\text{SiC}_3)$ and
			675m	$\nu_{\text{sym}}(\text{SiC}_3)$ and out-of-
			649w	phase vibrations
		654vw		
		631vw		
566w	572 (sh)			$\delta(\text{O-Si-O})$
		592m	584m	$\nu_{\text{sym}}(\text{Si-O-Si})$
		522w	534w	
537 (br, sh)	536(br)			Combination bands
490 (sh)	490 (sh)			
465m	468m			$\nu_{\text{sym}}(\text{Si-O-Si})$
		407w	463vw	Not assigned
			419m	
399s	401s			$\delta(\text{O-Si-O})$
	393 (sh)			

$C_2H_5SiCl_3$ which are skeletal modes of the ethyl group. On the other hand at least the 1064 cm^{-1} absorption can be interpreted in the same way as the 1213 cm^{-1} band.

Next the vibrations of the cubic siloxane cage are discussed. The crystal-structure determination shows that the siloxane cage can be approximated quite well by C_{3v} . This means that all T_{1u} vibrations split into A_1 and E and that some Raman and inactive modes of $H_8Si_8O_{12}$ become in principle IR active and split according to this symmetry reduction too. We have estimated the vibrational frequencies of the siloxane cage of $C_6H_{13}(H_7Si_8O_{12})$ based on a normal coordinate analysis of $CH_3(H_7Si_8O_{12})$ by applying the force field of $H_8Si_8O_{12}$ and an estimated Si-C force constant ($3.24 \times 10^{-8}\text{ N \AA}^{-1}$).⁶ This shows that the splitting between the E and the A_1 mode originating from the T_{1u} vibrations of $H_8Si_8O_{12}$ is small. It explains why the spectrum of $C_6H_{13}(H_7Si_8O_{12})$ remains simple in spite of the symmetry reduction. We therefore expect to observe such a splitting only in regions with narrow bands as e.g. for $\delta(\text{Si-H})$.

$2280\text{--}2200\text{ cm}^{-1}$. Only a broad band is found at 2274 cm^{-1} with $w_{\frac{1}{2}} = 30\text{ cm}^{-1}$ assigned to $\nu(\text{Si-H})$. It is striking that the Si-H stretching of $C_6H_{13}(H_7Si_8O_{12})$ and **2** are separated by about 70 cm^{-1} , although in both molecules the Si-H group has a very similar chemical environment. Inspection of the experimental data and molecular orbital calculations showed that this discrepancy is caused by the different H-Si-O-Si conformations of the two molecules. The cage structure of $H_8Si_8O_{12}$ allows only an *anti* H-Si-O-Si conformation while *syn* is the stable form of **2**.¹⁵

$1150\text{--}1000\text{ cm}^{-1}$. The band at 1139 cm^{-1} can be assigned to the antisymmetrical Si-O-Si stretching.⁶ Similar to the Si-H stretching one a band splitting according to the symmetry reduction has not been detected because of the large bandwidth of $w_{\frac{1}{2}} = 30\text{ cm}^{-1}$.

$960\text{--}800\text{ cm}^{-1}$. In $H_8Si_8O_{12}$ the $\delta(\text{Si-H})$ mode appears as a very narrow band at 881 cm^{-1} , while $C_6H_{13}(H_7Si_8O_{12})$ shows five intense absorptions between 916 and 847 cm^{-1} . A PED analysis of $H_8Si_8O_{12}$ showed between 932 and 862 cm^{-1} one T_{1u} IR, an E_g and a T_{2g} Raman and three inactive modes of symmetry type T_{1g} , E_u and T_{2g} , all of them bearing $\delta(\text{Si-H})$ character.⁶ After symmetry reduction to C_{3v} seven bands are expected to appear in this region, two additional modes are forbidden and one is shifted to lower energies. The possibility that one of the five detected vibrations belongs to a skeletal vibration of the organic substituent can be ruled out because the same intensity and absorption pattern was observed in $[\text{Co}(\text{CO})_4(\text{H}_7\text{Si}_8\text{O}_{12})]$.

$625\text{--}460\text{ cm}^{-1}$. The symmetric Si-O-Si stretching vibrations are expected in this region. In $H_8Si_8O_{12}$ this band appears at 465 cm^{-1} and the medium intensity band at 468 cm^{-1} is therefore assigned to this mode.

Finally there are the vibrations corresponding to O-Si-O deformations at 572 and 401 cm^{-1} which have no counterpart in the model substances **1** and **2**. That at higher energy loses much of its intensity compared to $H_8Si_8O_{12}$. The lowest-energy band shows a shoulder which is an additional indication of the symmetry reduction taking place on going from $H_8Si_8O_{12}$ to $C_6H_{13}(H_7Si_8O_{12})$.

Experimental

Chemicals.—Solvents were purchased from commercial sources and used as received. The compound $H_8Si_8O_{12}$ was prepared according to the method of Agaskar¹⁶ and recrystallized from hot cyclohexane; $\text{HSi}(\text{OSiMe}_3)_3$ was purchased from ABCR, Karlsruhe, Germany.

Synthesis and Crystallization of $C_6H_{13}(H_7Si_8O_{12})$.—Hexylheptahydrooctasilasesquioxane was synthesized according to the literature.⁷ The white product was crystallized by slow evaporation from nonane-dichloromethane (1:1) to give clear, colourless aggregated flakes.

Synthesis of $C_6H_{13}\text{Si}(\text{OSiMe}_3)_3$.—The compound $\text{HSi}(\text{OSiMe}_3)_3$ (2 cm^3 , 5.8 mmol) was dissolved in toluene (5 cm^3). Hex-1-ene (1 cm^3 , 7.6 mmol) and a H_2PtCl_6 solution ($60\ \mu\text{l}$, 0.01 mol dm^{-3} in Pr^iOH) were added in toluene (5 cm^3) and the mixture heated at reflux for 24 h under N_2 . After evaporation of the solvent a highly viscous liquid remained which was suspended in hexane (Romil Chemicals) and injected twice on a $600 \times 25\text{ mm}$ PolymerLab (pore size $50\ \text{\AA}$, particle size $10\ \mu\text{m}$) size-exclusion liquid chromatography column. IR: see Table 3. NMR (CDCl_3 , standard SiMe_4): ^1H (300 MHz), δ 0.09 (s, 27 H), 0.43 (m, 2 H), 0.89 (t, 3 H) and 1.20–1.42 (m, 8 H). Mass spectrum (70 eV): m/z 365 (7, $[M - \text{CH}_3]^+$), 295 (14, $[M - C_6H_{13}]^+$), 281 (37, $[M - C_6H_{13} - \text{CH}_3 + \text{H}]^+$) and 207 (100%, $[M - C_6H_{13} - \text{OSi}(\text{CH}_3)_3 + \text{H}]^+$).

Crystal-structure Determination and Refinement.—Details of the experiment and refinement are given in Table 4. The crystals were aggregated and an approximate prism was cut out of such an aggregate and mounted in a quartz capillary. Reflection data were collected on a STOE AED-2 four-circle instrument, using Mo-K α radiation. Lattice parameters were determined from least-squares refinement of setting angles for 20 reflections in the θ range $10.76\text{--}18.74^\circ$. Intensity variation was monitored every 240 min using 3 reflections. The total intensity loss amounted to 3.69% and was corrected for by linear interpolation. An absorption correction was made, employing a Gaussian quadrature numerical method. The final agreement for equivalent reflections, R_{int} , was 0.0154. The structure was solved by direct methods using SHELXS 86¹⁷ and a total of 251 parameters were refined with respect to F^2 by full-matrix least-squares refinement with SHELXL 92,¹⁸ refining anisotropic

Table 4 Experimental data for the X-ray crystal structure analysis

Molecular formula	$C_6H_{20}O_{12}Si_8$
M	508.94
Crystal dimensions/mm	$0.42 \times 0.62 \times 0.28$
Crystal colour, shape	Colourless, transparent flakes
Crystal system	Triclinic
Space group	$P\bar{1}$
$a/\text{\AA}$	7.7775(9)
$b/\text{\AA}$	7.9747(9)
$c/\text{\AA}$	18.033(2)
$\alpha/^\circ$	86.9410(13)
$\beta/^\circ$	79.443(9)
$\gamma/^\circ$	84.378(11)
$U/\text{\AA}^3$	1093.5(2)
T/K	291
Z	2
$D_c/g\text{ cm}^{-3}$	1.546
Radiation type ($\lambda/\text{\AA}$)	Mo-K α (0.710 73)
$\mu(\text{Mo-K}\alpha)/\text{mm}^{-1}$	0.540
Transmission factor range	0.7876–0.8504
$F(000)$	528
Scan type	ω -2 θ
θ Range/ $^\circ$	2.30–30.01
Index range	$-10 < h < 10$, $-11 < k < 11$, $0 < l < 25$
No. of unique data	6373
No. of observed data	2850
$[F_o^2 > 3\sigma(F_o^2)]$	
Final R for observed data ^a	0.0421
Final R' for observed data ^b	0.1121
Goodness of fit, S^c	1.168
Final difference-Fourier residuals, maximum and minimum/ $e\ \text{\AA}^{-3}$	0.38, -0.33
Largest and mean Δ/σ	< 0.001 , < 0.001

^a $R = \sum ||F_o| - |F_c|| / \sum |F_o|$; conventional R value based on $F_o > 4\sigma(F_o)$ observation criterion. ^b $R' = \{ \sum [w(F_o^2 - F_c^2)]^2 / \sum [w(F_o^2)^2] \}^{1/2}$ where $w = 1 / [\sigma^2(F_o^2) + (0.0505P)^2 + 0.67P]$, $P = [(F_o^2, 0)_{\text{max}} + 2F_c^2] / 3$. ^c $S = \{ \sum [w(F_o^2 - F_c^2)]^2 / (n - p) \}^{1/2}$ where n is the number of observations and p the number of parameters.

displacement factors for all non-hydrogen atoms. Hydrogen-atom positions were geometrically idealized with the Si-H distance¹⁹ restrained to 1.460(5) Å, and the C-H distances constrained to 1.97 (CH₂) and 1.96 (CH₃) Å respectively. The isotropic displacement of H(-Si) atoms was refined in one variable common to these seven hydrogen atoms, and likewise one variable was assigned to the hydrogen atoms on each of the six carbon atoms. Additional geometrical calculations were made with PLATON,²⁰ and the molecular illustrations with SHELXTL PLUS²¹ and SCHAKAL 92.²²

Additional material available from the Cambridge Crystallographic Data Centre comprises H-atom coordinates, thermal parameters and remaining bond lengths and angles.

IR Spectroscopy.—The IR transmission spectra were measured with a BOMEM DA3.01 FTIR spectrometer equipped with a liquid-nitrogen cooled MCT detector (500–5000 cm⁻¹) and a liquid-helium cooled CuGe detector (350–4000 cm⁻¹). A KBr beamsplitter was applied for measurements above 700 cm⁻¹, whereas in the range 350–700 cm⁻¹ a 3 µm Mylar beam splitter was used. The spectra of H₈Si₈O₁₂ and C₆H₁₃(H₇Si₈O₁₂) were measured in CCl₄ with a resolution of 0.5 cm⁻¹. The spectrum of H₈Si₈O₁₂ was interpolated between 720 and 840 cm⁻¹, whereas C₆H₁₃(H₇Si₈O₁₂) was measured in pentane in this region. The spectra of C₆H₁₃Si(OSiMe₃)₃ and HSi(OSiMe₃)₃ were measured in the same way as that of C₆H₁₃(H₇Si₈O₁₂).

Acknowledgements

This work is financed by the Schweizerischer Nationalfonds zur Förderung der wissenschaftlichen Forschung (project NF 20-34042.92) and by the Swedish Natural Science Research Council. We also thank the Schweizerisches Bundesamt für Energiewirtschaft for financial support (project BEW-EPA 217.307).

References

- 1 K. Larsson, *Ark. Kemi*, 1960, **16**, 215.
- 2 T. P. E. auf der Heyde, H. B. Bürgi, H. Bürgy and K. W. Törnroos, *Chimia*, 1991, **45**, 38.
- 3 H. B. Bürgi, K. W. Törnroos, G. Calzaferri and H. Bürgy, *Inorg. Chem.*, 1993, **32**, 4914.
- 4 K. W. Törnroos, H. B. Bürgi, G. Calzaferri and H. Bürgy, *Acta Crystallogr., Sect. B*, in the press.
- 5 P. A. Agaskar, V. W. Day and W. G. Klemperer, *J. Am. Chem. Soc.*, 1987, **109**, 5554.
- 6 M. Bärtsch, P. Bornhauser, G. Calzaferri and R. Imhof, *J. Phys. Chem.*, 1994, **98**, 2817.
- 7 G. Calzaferri, D. Herren and R. Imhof, *Helv. Chim. Acta*, 1991, **74**, 1278.
- 8 G. Calzaferri and R. Imhof, *J. Chem. Soc., Dalton Trans.*, 1992, 3391.
- 9 G. Calzaferri, R. Imhof and K. W. Törnroos, *J. Chem. Soc., Dalton Trans.*, 1993, 3741.
- 10 M. Morán, C. M. Casado, I. Cuadrado and J. Losada, *Organometallics*, 1993, **12**, 4327.
- 11 G. Koellner and U. Müller, *Acta Crystallogr., Sect. C*, 1989, **45**, 1106.
- 12 A. L. Smith, *Spectrochim. Acta*, 1960, **16**, 87.
- 13 D. Lin-Vien, N. B. Colthup, W. G. Fateley and J. G. Grasselli, *The Handbook of Infrared and Raman Characteristic Frequencies of Organic Molecules*, Academic Press, San Diego, 1991; N. B. Colthup, L. H. Daly and S. E. Wiberley, *Introduction to Infrared and Raman Spectroscopy*, Academic Press, San Diego, 1990.
- 14 H. Kriegsmann, *Z. Elektrochem.*, 1961, **65**, 336.
- 15 M. Bärtsch, G. Calzaferri and C. Marcolli, *Res. Chem. Interm.*, in the press.
- 16 P. A. Agaskar, *Inorg. Chem.*, 1991, **30**, 2707.
- 17 G. M. Sheldrick, *Acta Crystallogr., Sect. A*, 1990, **46**, 467.
- 18 G. M. Sheldrick, SHELXL 92, Test version. Program for the Refinement of Crystal Structures, University of Göttingen, Germany, 1992.
- 19 K. W. Törnroos, *Acta Crystallogr., Sect. C*, 1994, in the press.
- 20 A. L. Spek, PLATON 90, Vakgroep Algemene Chemie, University of Utrecht, The Netherlands, 1990.
- 21 G. M. Sheldrick, SHELXTL PLUS, Release 4.1 Siemens Analytical X-Ray Instruments Inc., Madison, Wisconsin, 1990.
- 22 E. Keller, SCHAKAL 92, A Program for the Graphic Representation of Molecular and Crystallographic Models, University of Freiburg, Germany, 1992.

Received 11th May 1994; Paper 4/02805H